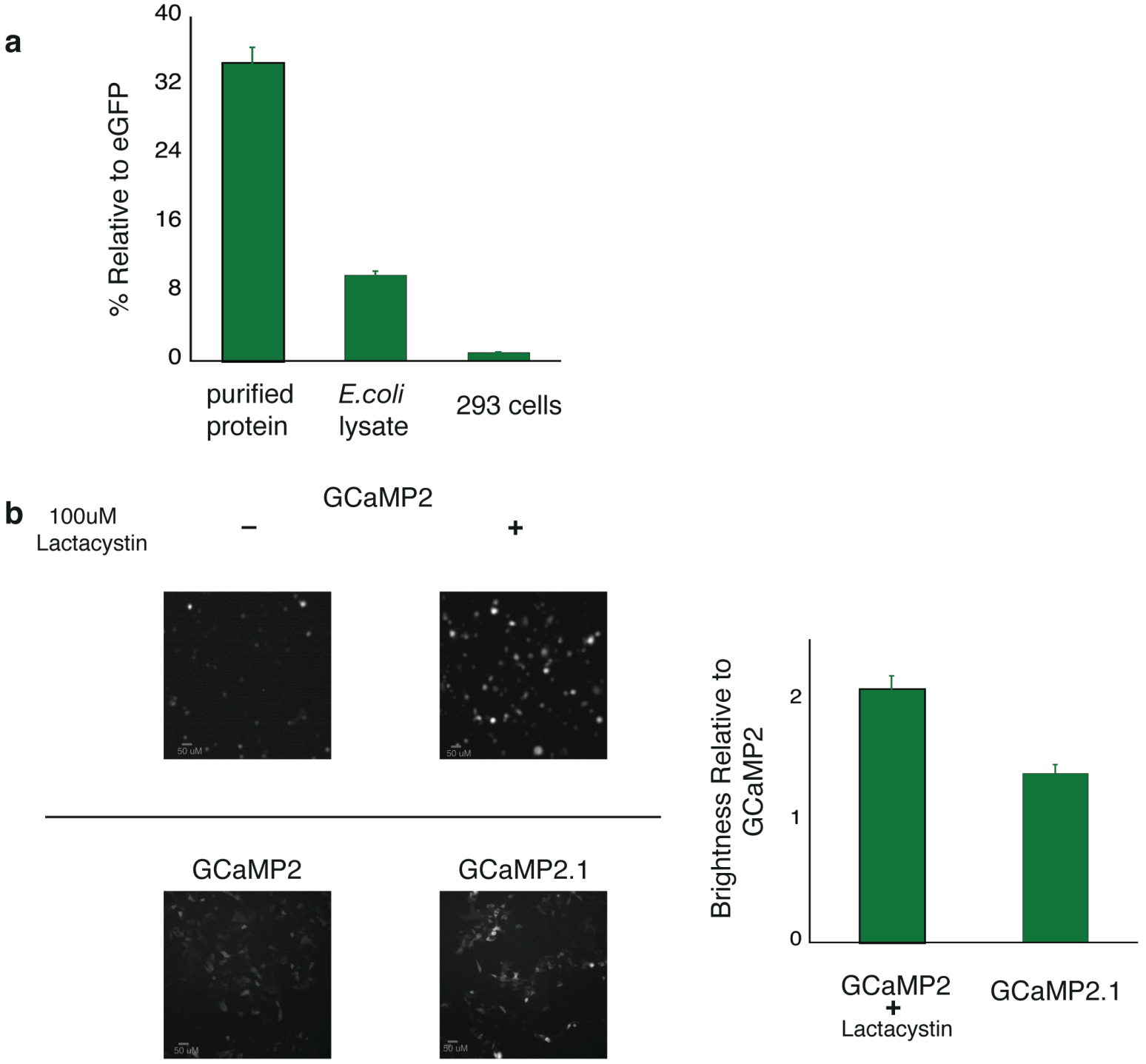

Supplementary Figure 1. Improving the protein stability of GCaMP2. **(a)** Comparison of baseline brightness in various biological systems. The fluorescence intensity was measured with 10 mM EGTA **(b)** Protein turn-over of GCaMP2 is mediated at least partially via the ubiquitin-proteasome pathway. Addition of lactacystin (top panel) or removing the N-terminal degron (bottom panel) increased the baseline brightness of GCaMP2. Error bars indicate standard deviation of the mean.

a

```
GCaMP2 MRGSHHHHHHGMASMTGGQQMGRDLYDDDDKDLATMVDSSRRKWNKTGHA      50
       VRAIGRLSSLENVYIMADKQKNGIKANFKIRHNIEDGGVQLAYHYQQNTP     100
       IGDGPVLLPDNHYLSTQSKLSKDPNEKRDHMVLLEFVTAAGITLGMDELY     150
       KGGTGGSMVSKGEELFTGVVPILVELDGDVNGHKFSVSGEGEGDATYGKL     200
       TLKFICTTGKLPVPWPTLVTTLTYGVQCFSRYPDHMKQHDFFKSAMPEGY     250
       IQERTIFFKDDGNYKTRAEVKFEGDTLVNRIELKGIDFKEDGNILGHKLE     300
       YNTRDQLTEEQIAEFKEAFSLFDKDGDGTITTKELGTVMRSLGQNPTEAE     350
       LQDMINEVDADGNGTIDFPEFLTMMARKMKDTDSEEEIREAFRVFDKDGN     400
       GYISAAELRHVMTNLGEKLTDEEVDEMIREADIDGDGQVNYEEFVQMMTAK*   450
```

b

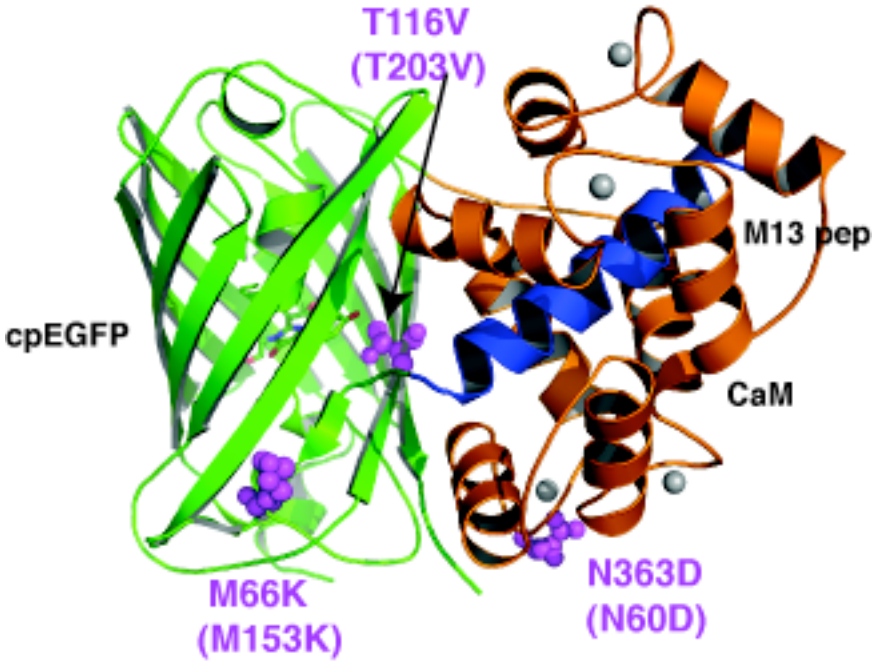

Supplementary Figure 2. Summary of positions where mutants were generated.

(a) Protein sequence of GCaMP2. The sites of side-directed mutagenesis are highlighted. Arginine at position 2 was deleted. Residues in red surround the

chromophore (highlighted in green). Residues in blue are known to contribute to GFP thermodynamic stability. Residues in pink are at the interface of M13 peptides and calmodulin (CaM). Residues in purple are responsible for the calcium-binding in EF-hands of CaM. **(b)** Structural model of GCaMP3, based on the structure of calcium-bound monomeric GCaMP2. The mutated amino acids are highlighted in purple.

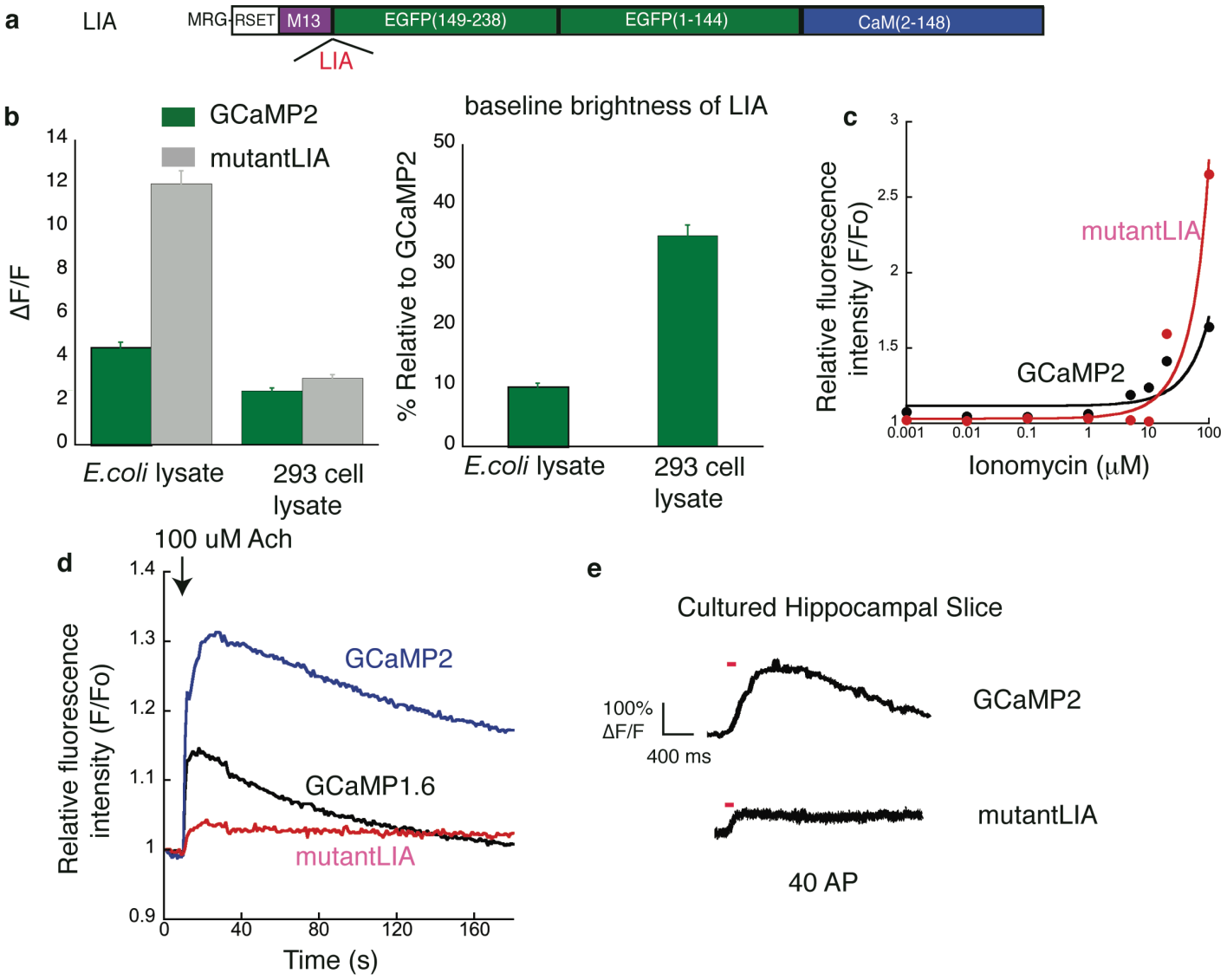

Supplementary Figure 3. Screening of GCaMP2 mutants in a HEK cell based assay.

The performance of mutants produced from this assay is closer to that in neurons than in purified protein.

(a) Schematic representation of mutant LIA structure.

The linker region between M13 and cpEGFP was mutated from amino acid "LE"

(Original translated XhoI site) to "LIA". **(b)** Signal change of GECIs is not consistent across various

biological systems. Initial semi-random mutagenesis in bacterial lysate found a variant (LIA) with huge

fluorescence change (left panel) and reduced baseline brightness (right), but the variant was unresponsive

in brain slice **(e)**. Error bars indicate standard deviation of the mean **(c)** LIA showed a better signal change than GCaMP2

in an ionomycin-based end point assay, but failed in a HEK293 cell-based assay with Ach-induced transient

calcium increases **(d)**. **(e)** Fluorescent changes of GCaMP2 and LIA in response to 40 APs in hippocampal slice.

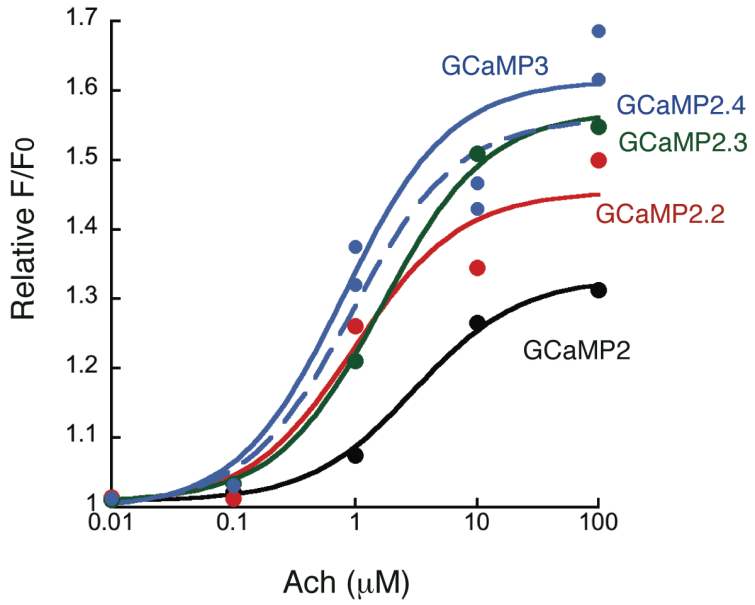

Supplementary Figure 4. Screening resulted in several mutants with improved baseline brightness and signal change in HEK 293 cells.

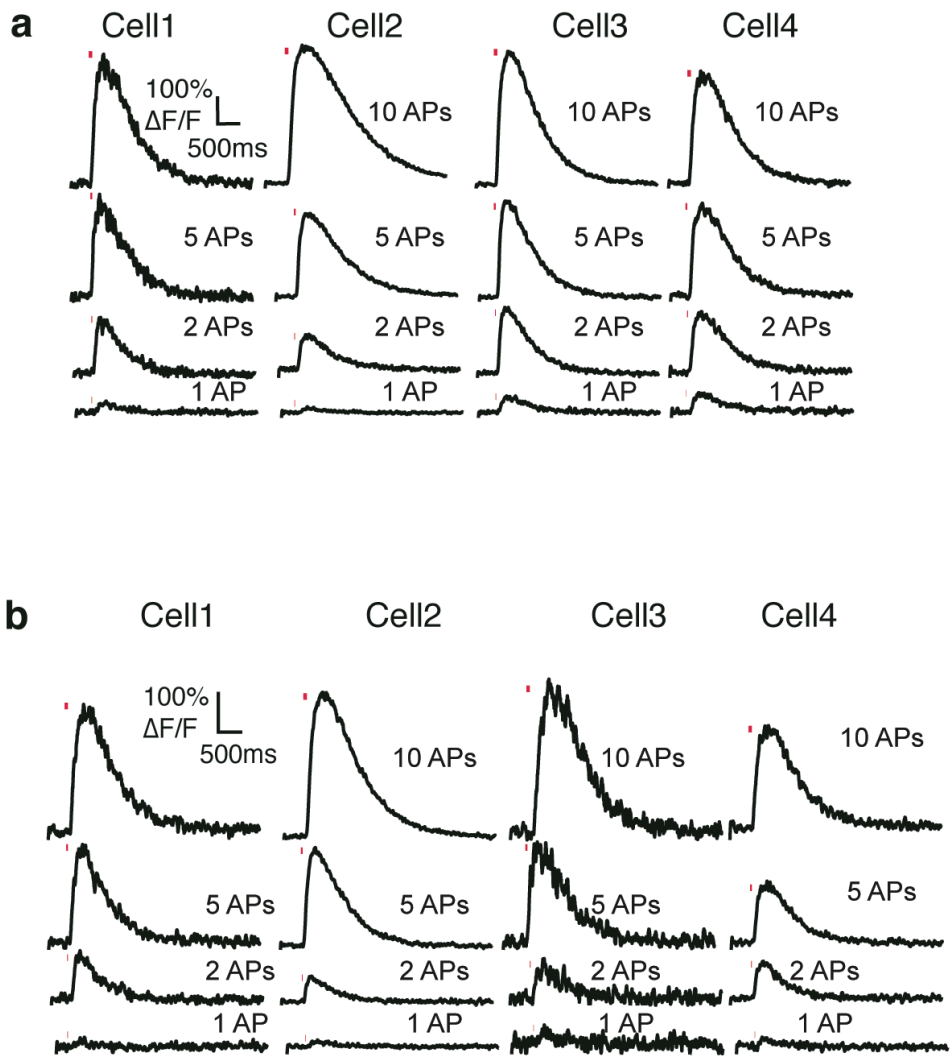

Supplementary Figure 5. Examples of single-trial responses of GCaMP3 in cultured hippocampal slice (a) and acute slice (b) from four neurons to 1, 2, 5, 10 action potentials evoked at 83 Hz.

For display, example traces were filtered with a Savitzky-Golay filter (2nd order, 30 ms).

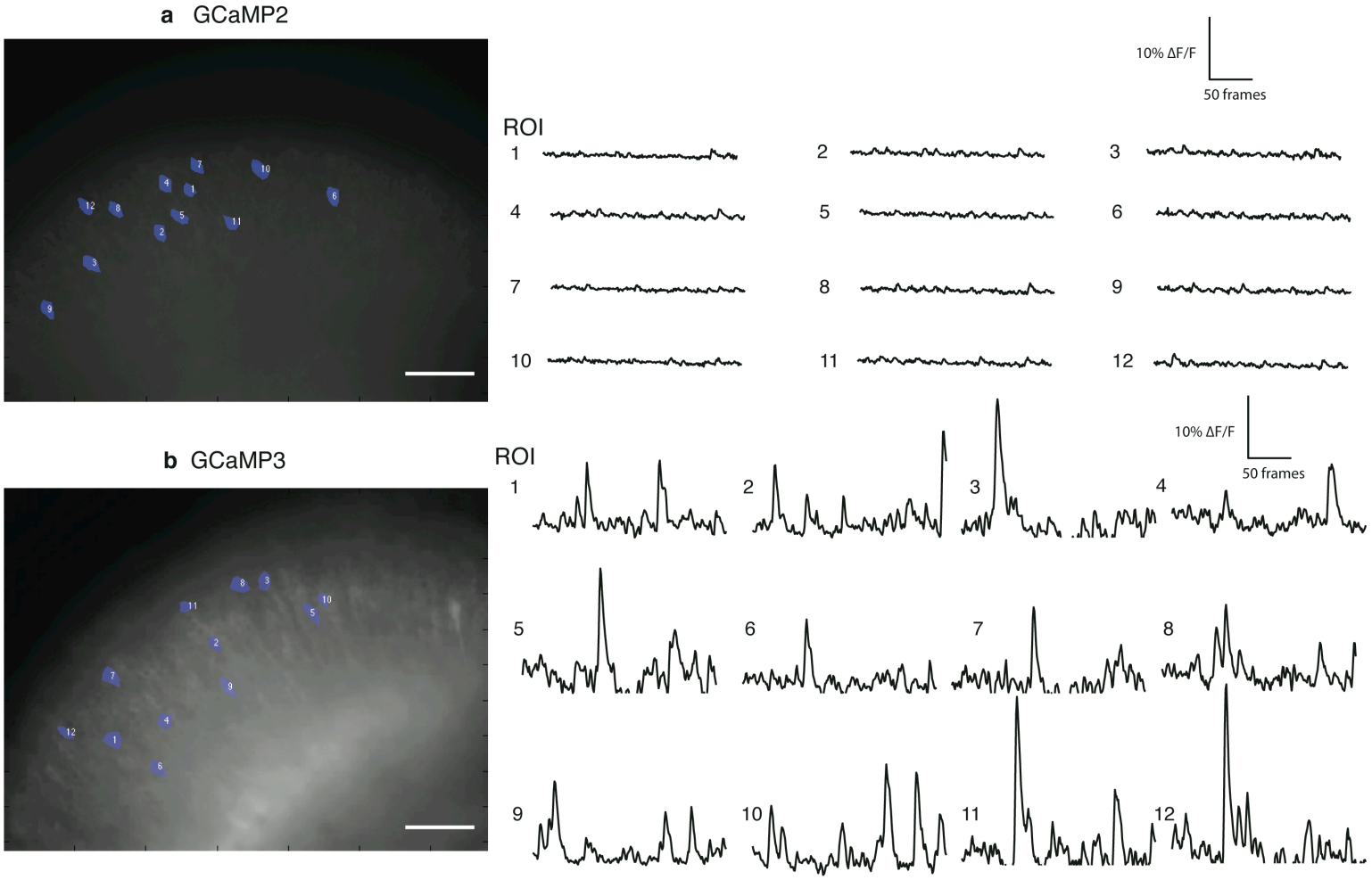

Supplementary Figure 6. Imaging spontaneous activity of neurons in hippocampal slice using GCaMP2 (a) and GCaMP3 (b). Scale bar, 200 μm.

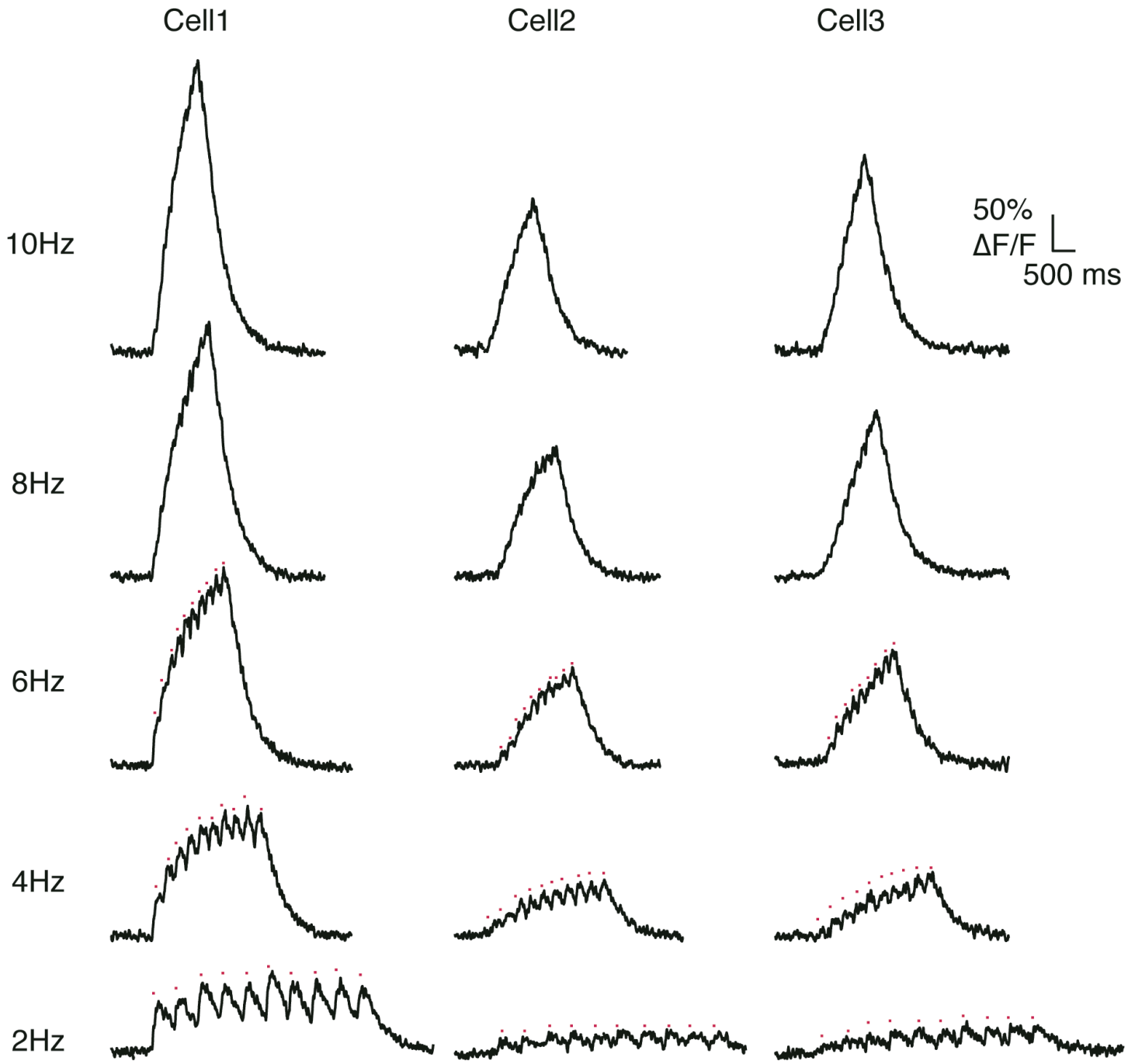

Supplementary Figure 7. Examples of single-trial fluorescence responses of GCaMP3 to low frequency stimuli from three cortical neurons. Action potentials were evoked at 2, 4, 6, 8 and 10 Hz respectively. Individual APs can be clearly resolved as high as 2 to 6 Hz. Peak fluorescence shown in red dots.

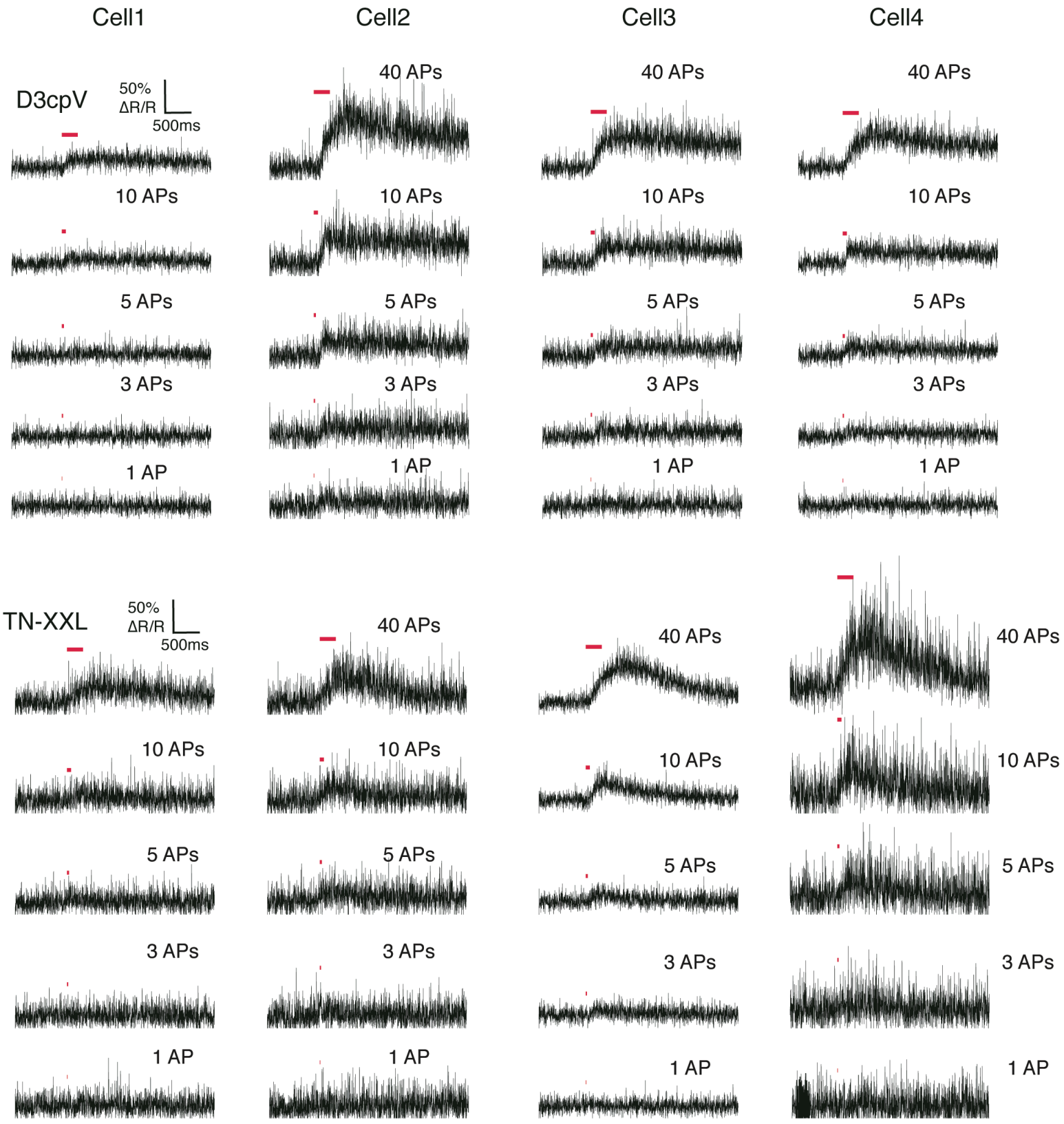

Supplementary Figure 8. Examples of single-trial responses of D3cpV (top panel) or TN-XXL (bottom panel) from four neurons to 1, 3, 5, 10 and 40 action potentials at 83 Hz.

For display, example traces were filtered with a Savitzky-Golay filter (2nd order, 25 ms).

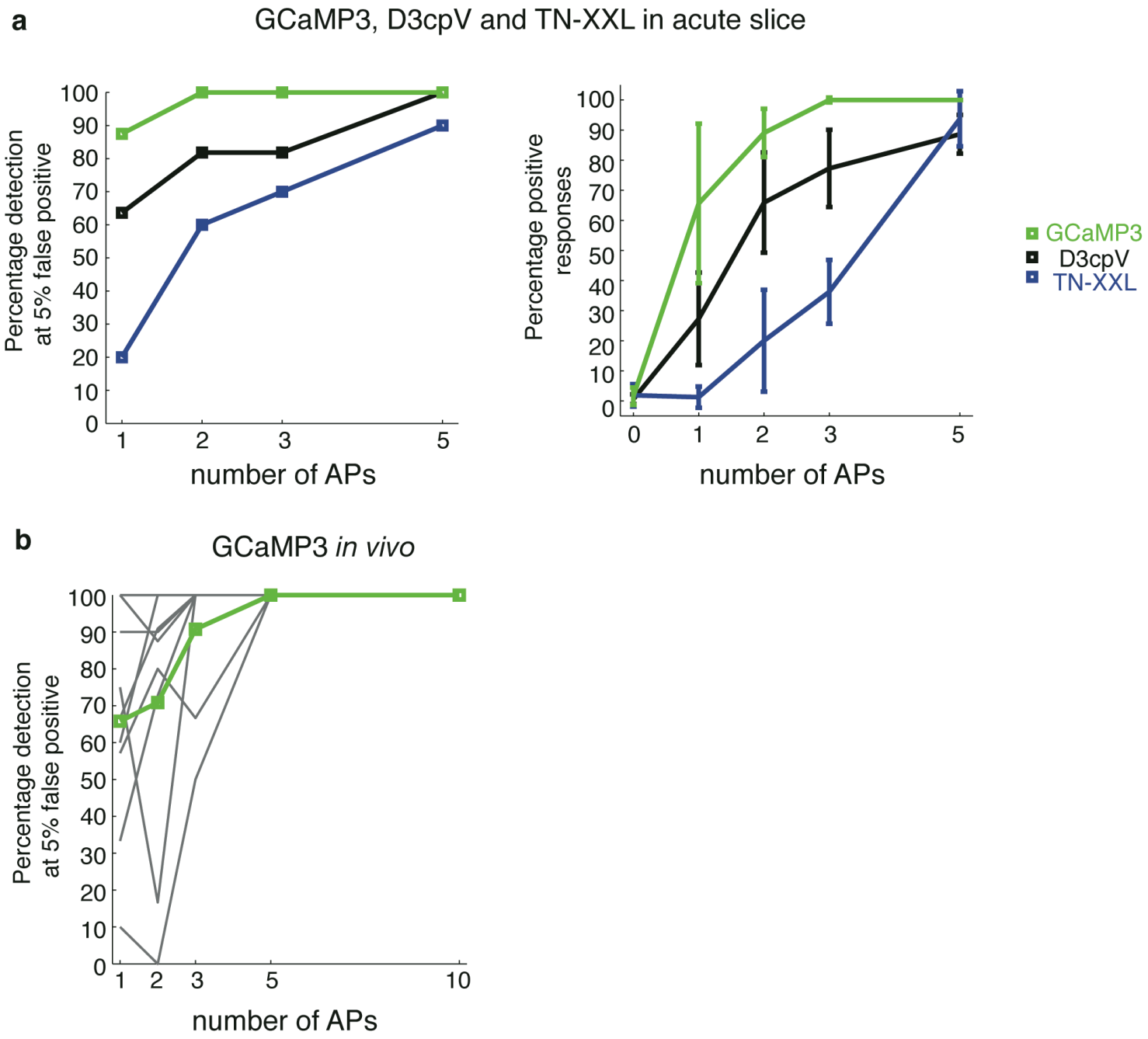

Supplementary Figure 9. Action potential detection probability. **(a)** Automated detection probability (see Methods) of GCaMP3, D3cpV and TN-XXL at given action potential trains at 83 Hz (left panel). Human blind-scoring detection probability of GCaMP3, D3cpV and TN-XXL (right panel). For blind-scoring test, the false positive rate is less than 2% (see detection probability at 0 AP). Error bars indicate standard deviation of the mean.

(b) Automated detection probability of GCaMP3 *in vivo* (n = 9 cells). Each neuron is shown in a thin gray line. The mean of 9 cells is shown in a thick green line.

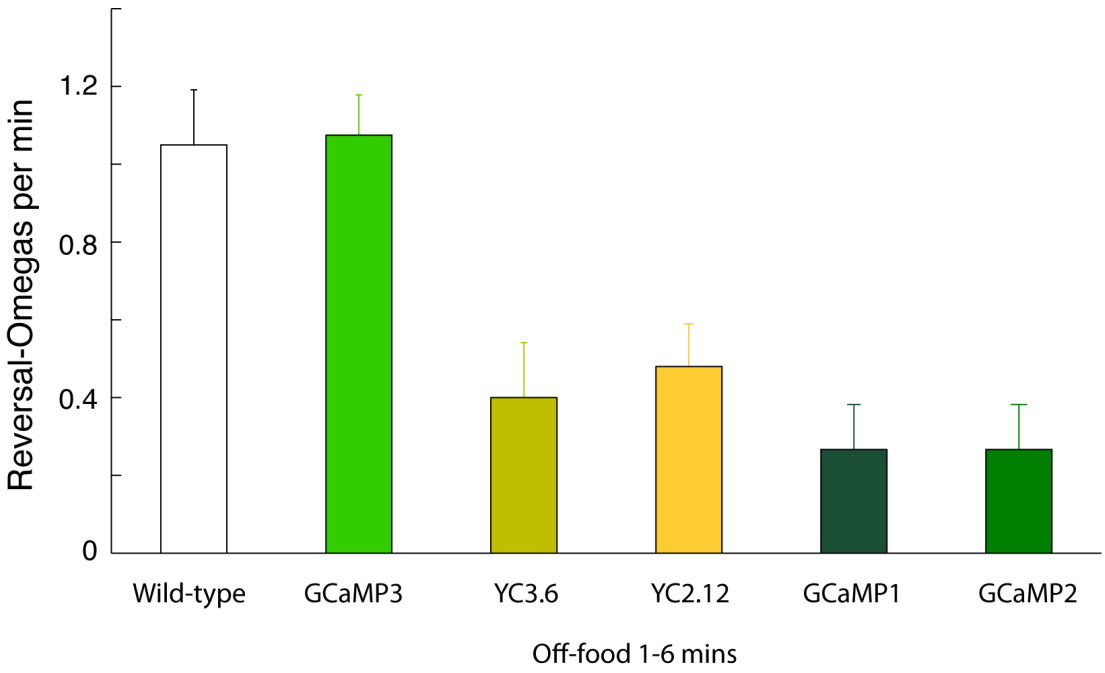

Supplementary Figure 10. ***C.elegans*** expressing GCaMP3 in AWC neurons showed similar local search turning behavior as wild-type animals. Decreased turning was observed in animals expressing YC3.6, YC2.12, GCaMP1 and GCaMP2 in AWC neurons. In *C.elegans*, local search turning behavior is triggered by AWC olfactory neurons, ASK gustatory neurons and AIB interneurons after they are removed from food. Here, animals of wild-type stain or AWC:GCaMP3 were first observed in food plates and then tranfered to a food-free plate. Animals were scored at 1-6 mins off food. Reversal-Omega, paired reversal-omega turning sequences. Error bars indicate standard deviation of the mean.

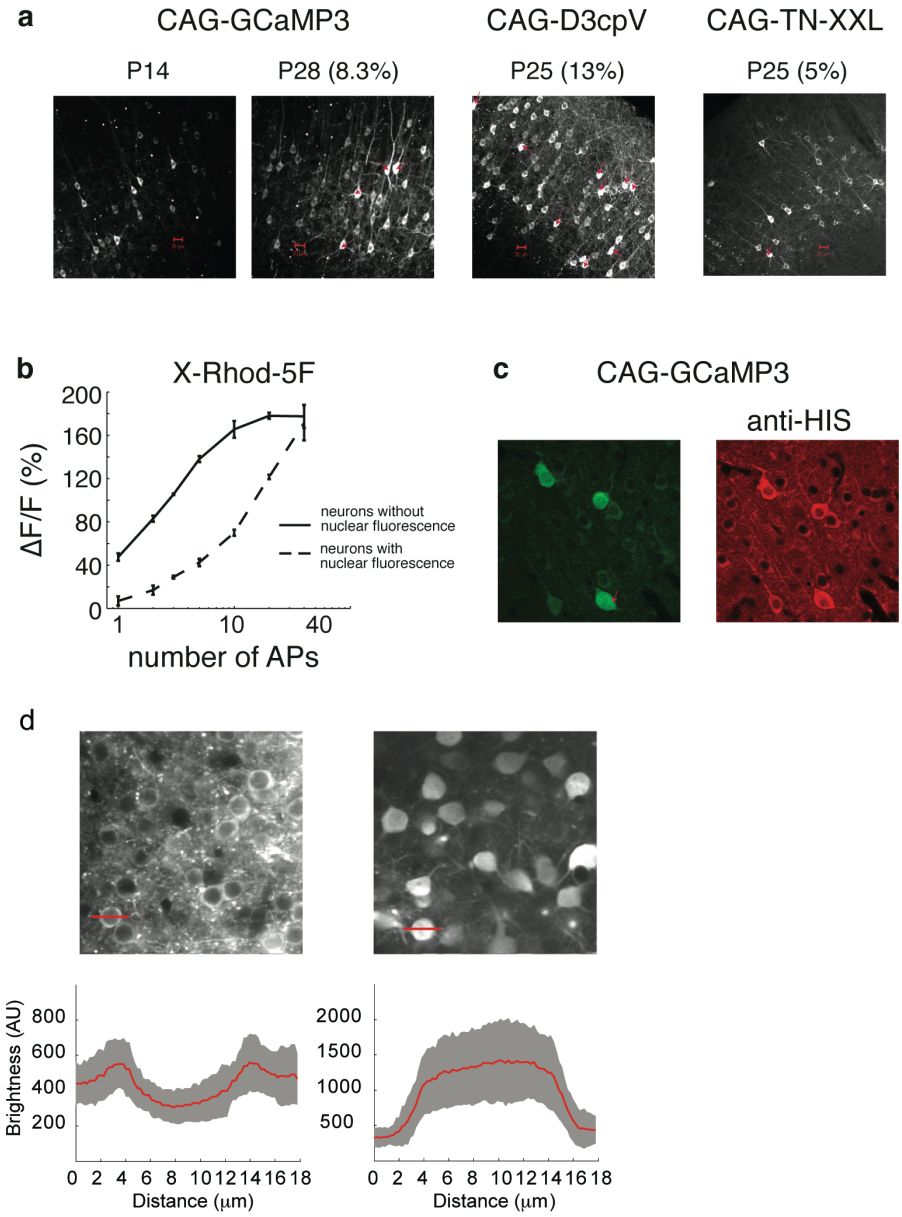

Supplementary Figure 11. Long-term expression of GECIs can cause altered neuron morphology and sensor properties. **(a)**. Expression of GECIs under control of the CAG promoter in layer 2/3 neurons of mouse cortex via in utero electroporation. At P25-P28, about 8.3% of GCaMP3, 13% of D3cpV and 5% of TN-XXL labeled neurons (indicated by red arrows) showed nuclear fluorescence. Scale bars show 20 μm. **(b)**. AP-evoked fluorescence response of X-Rhod-5F in neurons with nuclear fluorescence was attenuated. Error bars indicate standard deviation of the mean. **(c)**. Fluorescence intensity of GCaMP3 in neurons is correlated with the expression level of GCaMP3. HIS tag is present at the N-terminus of GCaMP3. An anti-HIS antibody preferentially labeled cytosolic GCaMP3. **(d)** Two-photon imaging section through cortical layer 2/3 with neurons infected with hsyn-GCAMP3 AAV. Cells where the fluorescence is restricted to the cytosol and excluded from the nucleus (left) are dimmer than those closer to injection site and with nuclear-filled fluorescence (right). Panel below shows the fluorescence intensity distribution through a cross section (mean in red and standard deviation in gray).

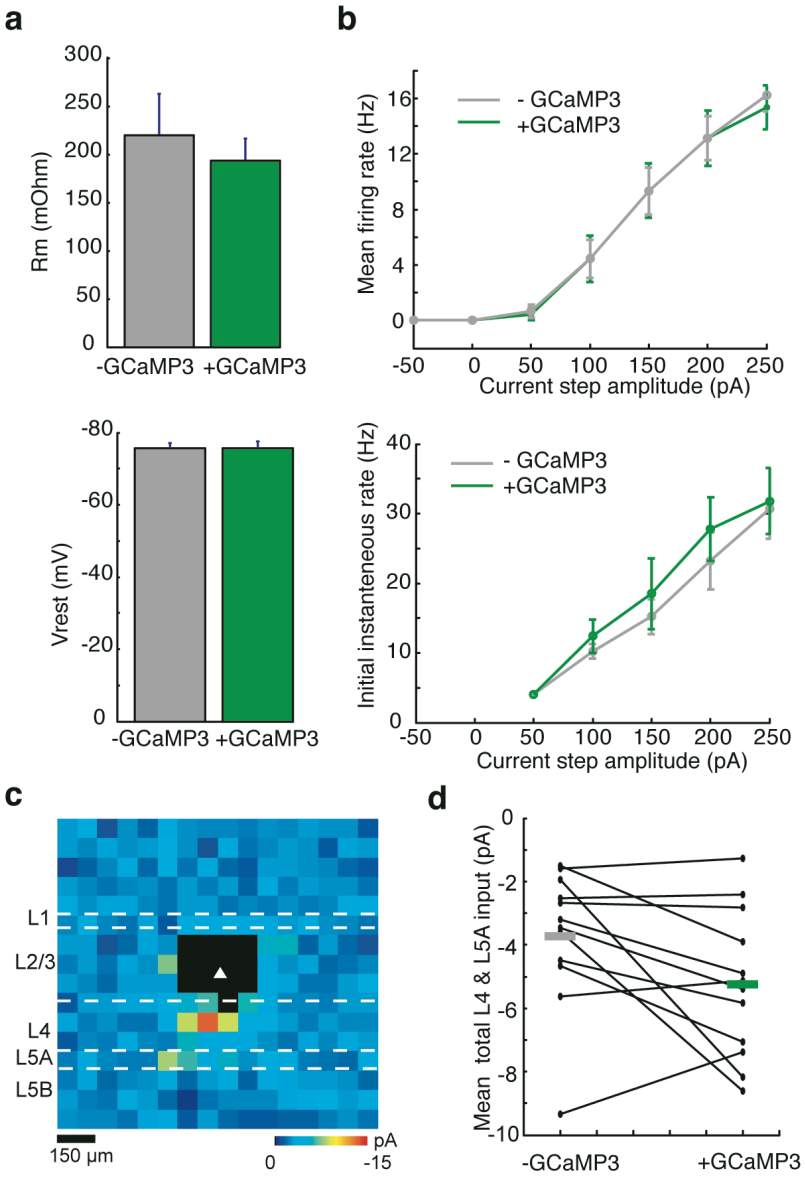

Supplementary Figure 12. Intrinsic and circuit properties of neurons with or without expression of GCaMP3 for 14-21 days. **(a)**. Input resistance (top) and resting potential (bottom) of GCaMP3 postive and negative L2/3 pyramidal neurons. (**b**). Firing properties of GCaMP3 positive (green) and negative (gray) L2/3 pyramidal neurons. Top, mean firing rates; bottom, initial instantaneous rate. Error bars indicate standard deviation of the mean. (**c**). Example of a synaptic LSPS input map for a single GCaMP3 expressing L2/3 pyramidal neuron (soma position is indicated by the triangle). Synaptic input maps measure the spatial distribution of synaptic input impinging onto L2/3 pyramidal neurons. Direct responses are blacked out. **(d)**. Total input from L4 and L5A for GCaMP3 negative and positive neurons. Pairs of neighboring cells recorded in the same experiment are joined by a line. The horizontal lines indicate group means (n.s., paired t-test, $p > 0.13$).

Sensor	Mutated Residues	*In vitro* Characterization	*In vivo* Characterization
GCaMP1			*C.elegans*
GCaMP1.6			*Drosophila*
GCaMP2	-	HEK293 cells, brain slice	
GCaMP2.1	ΔR2	HEK293 cells	
GCaMP2.2a	ΔR2 T116V(gfp T203V)	HEK293 cells, brain slice(data not shown)	
GCaMP2.2b	ΔR2 S118C(gfp S205C)	HEK293 cells, brain slice(data not shown)	*C. elegans* (data not shown)
GCaMP2.3	ΔR2 T116V(gfp T203V) M66K(gfp M153K)	HEK293 cells, brain slice(data not shown)	
GCaMP2.4	ΔR2 T116V(gfp T203V) N363D(cam N60D)	HEK293 cells, brain slice(data not shown)	*Drosophila*
GCaMP3	ΔR2 T116V(gfp T203V) M66K(gfp M153K) N363D(cam N60D)	*E. coli*, HEK293 cells, brain slice	*C. elegans* *Drosophila* Mouse cortex

.

Supplementary Table 1. Summary of the improved GCaMPs from HEK 293 cell-based screening. The improved GCaMP mutants showed better performance than GCaMP2 in various biological systems. GCaMP3 showed the largest signal changes among all variants and was further characterized in the sensory neurons of *Drosophila* and *C. elegans* and in the intact mouse brain.

Number of Action Potentials (APs)	ΔF/F % [mean±SD]				Signal to Noise [mean±SD]			
	GCaMP3	GCaMP2	D3cpV	TN-XXL	GCaMP3	GCaMP2	D3cpV	TN-XXL
0AP	3.5±2.1	2.9±2.3	2.9±2.1	3.8±2.0	1.5±1.0	1.9±1.4	1.8±1.3	1.9±0.9
1AP	14±2.7	3.6±2.3	5.0±3.0	4.2±2.1	6.1±1.2	2.3±1.5	3.0±1.6	2.3±1.2
2APs	59±34	9.3±8.8	7.7±3.5	6.5±3.5	26±15	6±5.7	4.7±2.1	4.0±1.9
3APs	113±45	18±20	9.5±4.9	6.4±3.0	50±20	11.7±12.9	5.8±3.0	3.5±1.7
5APs	215±75	33±32	13±5.8	13±6.7	94±33	21±21	8.0±3.6	7.1±3.7
10APs	373±196	40±40	20±10	22±10	164±86	26±16	13±6.2	12±5.6
20APs	450±240	113±90	32±16	36±15	198±105	73±58	19±10	20±8.1
40APs	505±224	278±84	43±22	49±16	239±136	179±54	26±13	27±9.0

Supplementary Table 2. Comparing GCaMP3 with GCaMP2 and the FRET-based sensors D3cpV and TN-XXL in layer 2/3 cortical neurons *via in utero* electroporation. The average fluorescence changes and signal to noise ratio of the GECIs following trains of action potentials are shown.

Sensor	% Transgenic lines showing defective local search turning behavior
GCaMP1	75
GCaMP2	33
YC2.12	60
YC3.6	50
TN-XXL	No signal in CFP channel
GCaMP3	0

Supplementary Table 3. Expression of Genetically-encoded calcium indicators in AWC neurons of *C. elegans* can lead to defective local search turning behaviors in some transgenic lines. However, none of transgenic lines expressing GCaMP3 in AWC neurons showed defective local search turning behavior after food removal.

Supplementary Movie 1

Spontaneous neural activity visualized by GCaMP2 in cultured hippocampal brain slice (3x real-time). The fluorescence traces were shown in Supp. Fig. 6a.

Supplementary Movie 2

Spontaneous neural activity visualized by GCaMP3 in cultured hippocampal brain slice (3x real-time). The fluorescence traces were shown in Supp. Fig. 6b.

Supplementary Movie 3

Naturally occurring activity of populations of layer 2/3 neurons expressing GCaMP3 in the primary motor cortex (M1) of awake, behaving mouse during 140 sec sequence of two-photon images (10X real time). The outlined neurons on the first frame correspond to the fluorescence traces in Fig. 6g.